Journal of Scientific Research and Development 1 (2): 7-14, 2014
Available online at www.jsrad.org
ISSN 1115-7569

Road machine as a prerequisite in today world road development

Akmetzhan Aliyev, Alisher Aliyev and Alnura Iskakov
D. Serikbayev East Kazakhstan State Technical University,
Ust-Kamenogorsk, Kazakhstan

Abstract: The method of defining the power, consumed by a planetary vibroexciter, allowing with the help of three-dimensional diagrams, to select basic parameters of elliptic planetary vibroexciter by a rational way at the stage of its design has been presented. This can provide the increase of effectiveness and substantial reduction of energy capacity. To build up-to-date highways it is necessary to have road-making machines, which differ from the traditional ones with not only their design and comfort, but also having innovating mechanisms and working in accord with new technologies. Road vibrating rollers are related to such machines. They use planetary vibroexciters in their construction for sealing road-building materials. Planetary vibroexciters with elliptic toe cams, generating excitement of centrifugal along with Coriolis forces, combined effect of which provides several increase of integral force of directed driving force relate to the new developments, providing substantial intensification of the toe cam process. Method of determining and analysis of critical angles of slipping of inertial runner on the surface of elliptic inner race with the help of three-dimensional diagrams built with MathCAD software.

Key words: Planetary vibroexciter • Elliptic • Runner • Sliding • Axis

INTRODUCTION

Dynamic analysis of elliptic planetary vibroexciter has determined the basic force dependences of shaking force and resistance forces to rotation spider [1, 2] and from the point of view of energy intensity it implies the mechanism force calculation in the whole, without dividing it into structural groups and also calculation of active forces and resistance forces without participating of forces of inertia.

Calculating scheme of a vibroexciter with central position of the spider axe is presented on Figure 1.

On the calculation scheme frictional moment of rolling is presented as a pair of forces with the lever "h":

$$h = r \cdot \sin\delta \tag{1}$$

As all shown on the design diagram forces are variable, we will use the following dependence for determining supplied power:

$$P_{sum} = \left[\sum (M_O(F_i) + M_{TP}^O - M_{TP}^C)\right] \cdot \omega \tag{2}$$

where $\sum M_{O(F_i)}$ is sum moment of all specified forces relatively to the spider rotation axis O.

$$\sum M_O(F_i) = \begin{cases} \begin{bmatrix} -G_1 \times x_{S1} - G \times r \times \cos\varphi - \\ -F_\tau \times r \times \cos\delta + N \times (h-k) \end{bmatrix}, if\ \delta \rangle 0 \\ \begin{bmatrix} -G_1 \times x_{S1} - G \times r \times \cos\varphi - \\ -F_\tau \times r \times \cos\delta + N \times (h+k) \end{bmatrix}, if\ \delta \langle 0 \\ \begin{bmatrix} -G_1 \times x_{S1} - G \times r \times \cos\varphi - \\ -F_\tau \times r \times \cos\delta + N \times k \end{bmatrix}, if\ \delta = 0 \end{cases} \tag{3}$$

In the process of movement of the inertial runner on the inner race may be observed as pure rolling and also as rolling with sliding or skidding [3]. In terms of said above, one may conclude, that supplied power is a variable quantity [4].

Dependence (2) allows to determine the power consumed for getting necessary driving force and expenditure of energy; and also to determine the power of the engine at designing computation.

Critical parameters of asymmetric planetary vibroexciter with elliptic inner race include:

Corresponding Author: Akmetzhan Aliyev

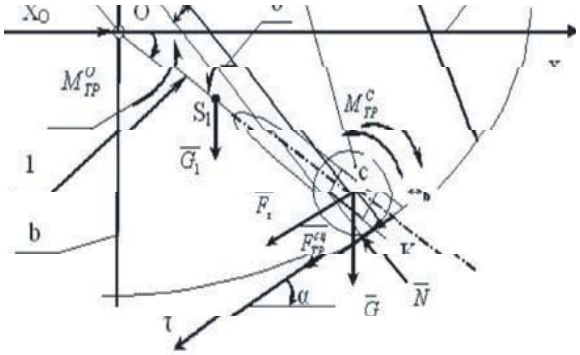

Fig, 1: Design diagram of the planetary vibroexciter with elliptic inner race and central position of the spider axis.

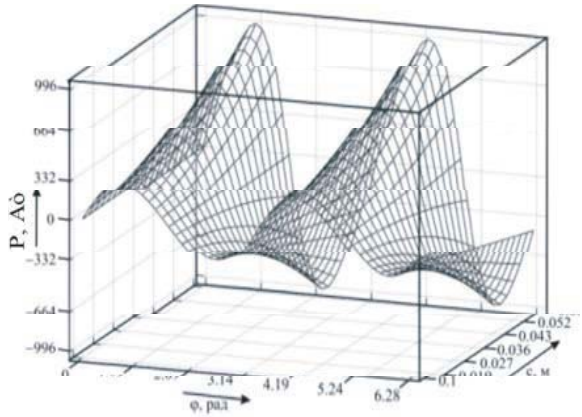

Fig. 2: Diagram of supplied power of the planetary vibroexciter in the function of the spider angle of rotation f and focal length "c"

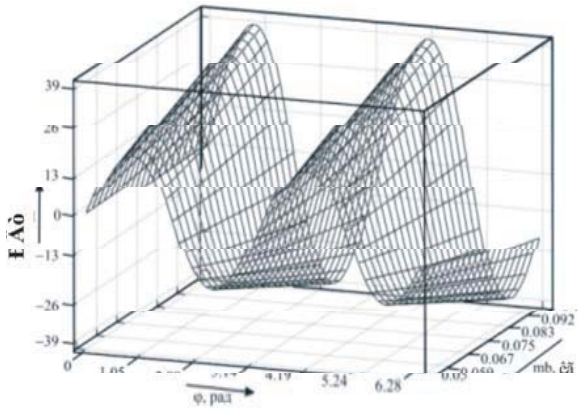

Fig. 3: Diagram of supplied power of elliptic vibroexciter in the function of the spider angle of rotation φ and mass of the runner m_b

eccentricity of elliptic inner race; mass of inertial runner and angular frequency (rate of the spider rotation ω) of vibrations [5].

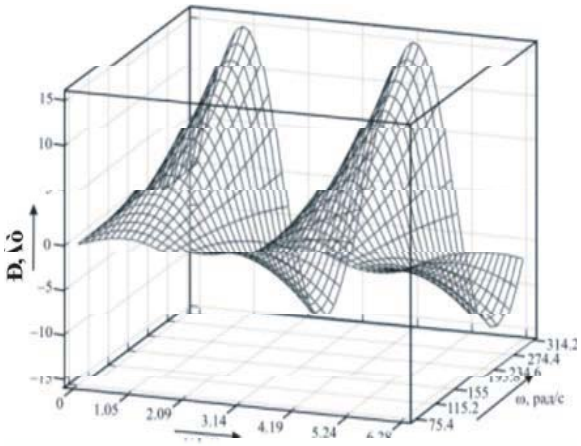

Fig. 4: Diagram of supplied power of the vibroexciter in the function of the spider angle of rotation φ and angular frequency of vibrations ω.

To follow the tendency of changing of dynamic parameters of elliptic vibroexciter, we will calculate the consumed power using the diagram of the vibroexciter with central position of the spider axis (Figure 1) and parameters for the calculating: axle of ellipse a=0,075m, b=0,05m; coefficient of kinetic friction - f_{sc}=0,2; changing of focal distance of elliptic inner race changes in the range - c = 0,01- 0,06; mass of the runner - m_b = 0,05 - 0,095 kg; angular frequency of vibrations ω = 76,4 - 314,2 s^{-1}.

Angle of the spider rotation φ changes clockwise in the range of 0<φ<360°.

All dependences and raw data of the work process of elliptic planetary vibroexciter were processes on PC in Mathcad media, in the result of which we got diagrams of supplied power for the vibroexciter driver depending upon changing of its critical parameters and the spider angle of rotation φ.

For example, the diagram, presented on Figure 2, allows to follow the tendency for growth of the supplied energy with the increasing of focal length (1.6 times increasing of focal length leads to 1.7 times increase of supplied energy), which is explained by the growth of dissipative losses while rounding by the inertial runner the sites of inner race, where the current radius of the rotation axis of runner C is of extreme values.

Analyzing the diagram of supplied power on Figure 3, we come to the conclusion that 1.5 times increase of the runner mass leads to 1.4 increase of supplied power.

To determine the influence of angular frequency of vibrations ω on supplied power we will look at the diagram on Figure 4, analysis of which shows that

1.3 times increase of angular frequency vibrations leads to 2.4 increase of supplied power. Further 1.5 times increase of frequency leads to 3.4 times disproportionate increase of power, which can be explained by the increase of dissipative losses in kinematic pairs and also by the fact that centrifugal forces of inertia of the vinbroexciter definite sections are in quadratic dependence upon angular frequency of vibrations.

Necessary compaction of soil, crushed stone and asphalt-concrete in the road branch is not only a component of the technological process of making a road bed, bedding and surface, but also serves as actually main operation to provide their strength, stability and durability.

The main means of compaction of asphalt-concrete mixtures are vibrating and combined rollers, additionally equipped with rubber-mounted and smooth-rolling static-weight rollers.

The working part of a vibroroller is a metallic roll of hollow-core welded construction, inside of which there is a built-in vibroexciter, being a source of shaking force, transferred on the roll and exciting driving force, that introduces the system “roller – compaction material” into oscillatory motion.

One of the effective methods of increasing of compaction machines efficiency is the use of asymmetrical vibroexciters of planetary type. Their inertial runner changeable angle rate relating to the center of the inner race arc is provided with the axis eccentricity of the spider rotation relatively to the arc center or non-circular form of the inner race. Meanwhile, the runner makes complicated plane-parallel movement [6].

Vibroexciter, from the point of view of the process of road-building materials compacting is the central element of the system, effecting all other subsystems. This is also true for the case when it is set in the roll of a road roller. Major parameters of the vibroexciter is the sum driving force, frequency and vibrational amplitude, as well as power supply of the working process, that is, consumed power of the drive.

Since there are practically no study of elliptic planetary vibroexciters in scientific literature, we will investigate the working process of a planetary vibroexciter with elliptic inner race and make its brief dynamic analysis for three different settings of the spider axis: in the center of symmetry, in the left and right focus of the elliptic inner race. For the sake of clearness, we will make practical calculating for one of experimental models with the following parameters: the runner mass m_b=0,06597; sliding friction coefficient f=0,2; rooling

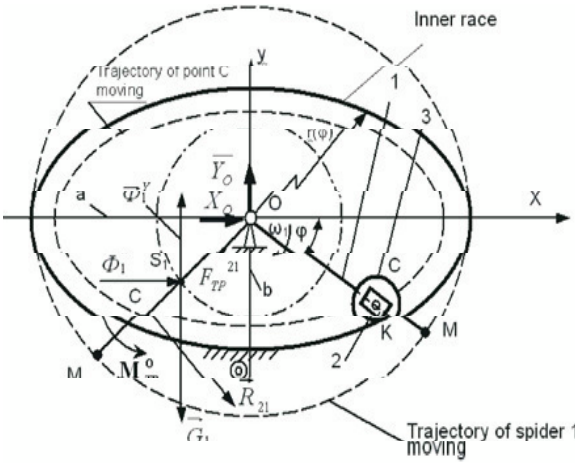

Fig. 5: Design diagram for dynamic analysis of the planetary vibroexciter with elliptic inner race at the central position of the spider.

friction coefficient k=0,00002; pivot bolt radius r_C=0,0015; runner radius r_b=0,015; mass of the spider m_K=0,3788. values are given in SI units.

For the calculating scheme we accept the following assumptions:

- Body and links of kinematic chain of a vibroexciter are rigid;
- There are no clearances in movable links;
- Links, as parts of a vibroexciter, are made and arranged ideally accurately;
- All angles are counted anticlockwise;
- Inertial runner (roller) uniform disk;
- Center of gravity of the spider is in the middle of its length L.

Design diagram for dynamic analysis of the elliptic planetary vibroexciter is presented on Figure 5.

The system of forces, presented on Figure 5, relates to plane optional and allows to equate three equations of equilibrium [6], solving which we find three force factors: X_O,Y_O and R_{21}.

Sum of projections on axis X, where centrifugal force of the runner inertia is presented as projections Φ^X and Φ^Y:

$$\sum F_X = X_O + ?_1^X + R_{21} \cdot \sin\varphi - F_{TP}^{21} \cdot \cos\varphi = 0 \qquad (4)$$

Sum of projections on axis Y:

$$\sum F_Y = Y_O + \Phi_1^Y - R_{21} \cdot \cos\varphi + F_{TP}^{21} \cdot \sin\varphi = 0 \quad (5)$$

Sum of moments of forces, relative to point *O*:

$$\sum M_O = -M_{TP}^O + R_{21} \cdot r - G_1 \cdot x_{S1} + \Phi_1^X \cdot y_{S1} - \Phi_1^Y \cdot x_{S1} = 0 \quad (6)$$

Solving equations 4 and 5 relatively to unknown, we find [7]:

$$X_O = F_{TP}^{21} \cdot \cos\varphi - \Phi_1^X - R_{21} \cdot \cos\varphi \quad (7)$$

$$Y_O = -F_{TP}^{21} \cdot \sin\varphi - \Phi_1^Y + R_{21} \cdot \sin\varphi \quad (8)$$

$$R_{21} = \frac{M_{TP}^O + G_1 \cdot x_{S1} - \Phi_1^X \cdot y_{S1} + \Phi_1^Y \cdot x_{S1}}{r} \quad (9)$$

F_{τ} - tangential component of driving force:

$$F_\tau = -G \cdot \cos\varphi - \Phi^Y \cdot \cos\varphi - \Phi^X \cdot \sin\varphi + R_{12} \quad (10)$$

N – normal reaction from the part of the inner race:

$$N = G \cdot \sin\varphi + \Phi^Y \cdot \sin\varphi - \Phi^X \cdot \cos\varphi \quad (11)$$

Projections of driving forces on coordinate axes:

$$\begin{cases} N_X = -N \cdot \cos\varphi + F_\tau \cdot \sin\varphi \\ N_Y = N \cdot \sin\varphi - F_\tau \cdot \cos\varphi \end{cases} \quad (12)$$

where

N_X - projection of driving force on axis *X*;
N_Y - projection of driving force on axis *Y*.

To follow the tendency of changing dynamic parameters we will examine the influence of geometric parameters on the basic dynamic characteristics on the example of experimental model of the planetary vibroexciter with elliptic inner race for the case of central position of the spider axis [7], taking three values of eccentricities of the elliptic inner race: e_1=0,507; e_2=0,6 and e_3=0,8.

Having calculated focal lengths for three pointed eccentricities using the formula $c = a.e$, where: is eccentricity of the elliptic inner race, we receive: c_1=0,038; c_2=0,045 and c_3=0,06.

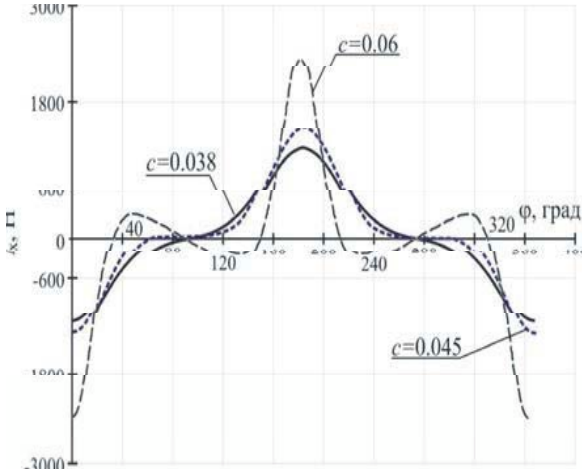

Fig. 6: Diagram of dependence of the vibroexciter driving force projection on abscissa axis for three different eccentricities of elliptic inner race: c_1=0,038; c_2=0,045 and c_3=0,06

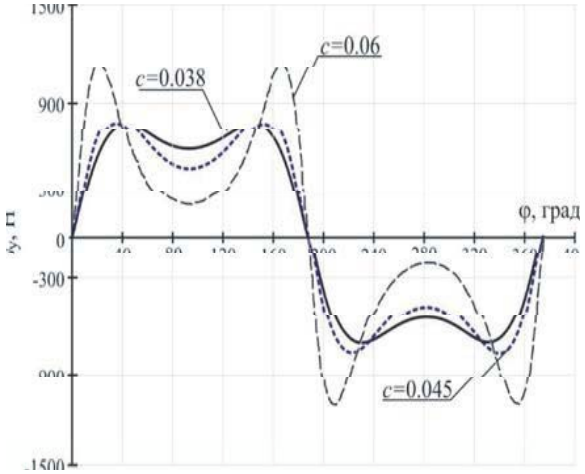

Fig. 7: Diagram of dependence of the vibroexciter driving force projection on ordinate axis for three different eccentricities of elliptic inner race: c_1=0,038; c_2=0,045 and c_3=0,06

Using equations presented above (4 – 12) we will draw comparative diagrams of driving force projections dependence for three values of focal lengths (Figures 6 and 7).

To make complete analysis of the vobroexciter parameters, we will use MathCAD software product, which allows to overlap a few linear diagrams in one, that is three-dimensional plotting. The diagrams can rotate in space, can be plotted in changing colors or with graticule overlay. Volumetric dependences shown on Figures 4 and 5, which analogs are diagrams of Figures 6 and 7, can serve as examples of such plottings.

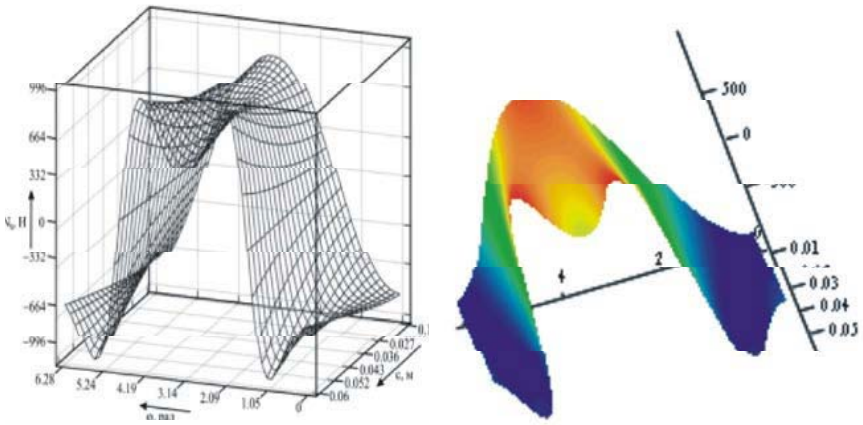

Fig. 8: Diagrams of the vibroexciter driving force projection on abscissa axis in the function of the spider turning angle φ and focal length "c"

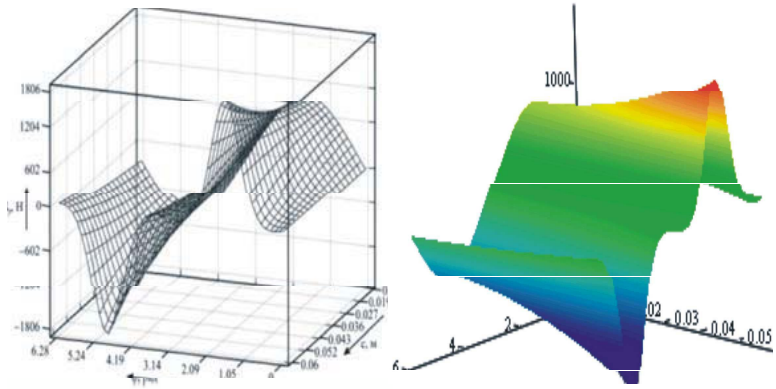

Fig. 9: Diagrams of the vibroexciter driving force projection on ordinate axis in the function of the spider turning angle φ and focal length c.

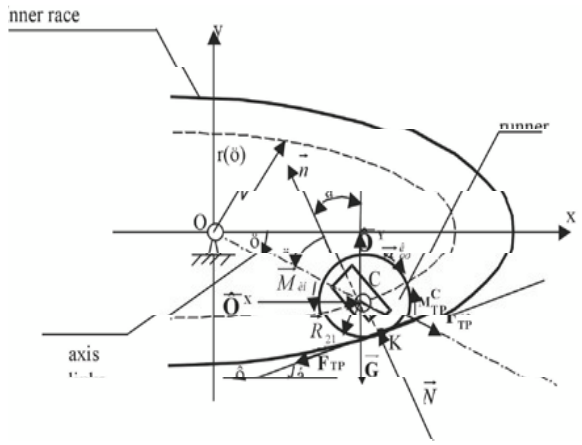

Fig. 10: Design diagram of the planetary vibroexciter with elliptic inner race

Analyzing diagrams, shown on Figure 8, one can notice the tendency to decreasing the period of vibrations of driving force projection on abscissa axis, at increasing of focal length more than 0.045, which was unsighted when we analyzed the plane diagram (Figure 6) and points at undisputed advantage of three-dimensional diagrams when we analyze the dynamic characteristics of the vibroexciter.

The main drawback of planetary vibroexciters including those with elliptic inner race is slippage of inertial runner on the surface of the inner race on certain parts of the path. It happens in the result of unparallelism of lines of centrifugal force effect with respect to regular reaction from the part of inner race (angle δ, Figure 10) and formation of inertial runner's own spontaneous moment [8].

To determine true effectiveness of the elliptic planetary vibroexciter it is necessary to find angular coordinates of slippage sites within the circular path of the runner movement. The task of the research is determining critical value of the spider turning angle φ_{cr} [9], under which the slippage of the inertial runner on the inner race starts and finishes.

We will analyze the conditions of the inertial runner rolling on the inner race. We will do that with the help of dynamic characteristics [9, 10], determined earlier:

Sun of projections on the axes X and Y:

$$\sum F_X = X_O + \Phi_1^X + R_{21} \cdot \sin\varphi - F_{TP}^{21} \cdot \cos\varphi = 0 \quad (13)$$

$$\sum F_Y = Y_O + \Phi_1^Y - R_{21} \cdot \cos\varphi + F_{TP}^{21} \cdot \sin\varphi = 0 \quad (14)$$

Sum moment of forces, with respect to the point O:

$$\sum M_O = -M_{TP}^O + R_{21} \cdot r - G_1 \cdot x_{S1} + \Phi_1^X \cdot y_{S1} - \Phi_1^Y \cdot x_{S1} = 0 \quad (15)$$

As point C of the runner center makes curvilinear motion, we take Euler's moving coordinates the starting point of which we overlap with the point K (Figure 10) for calculating the runner movement.
Sum of projections on normal axis n:

$$\sum F_n = N - G \cdot \cos\alpha + \Phi^Y \cdot \cos\alpha \mp F_{TP}^{12} \cdot \cos\delta - R_{12} \cdot \sin\delta - \Phi^X \cdot \sin\alpha = 0, \quad (16)$$

Sum of projections on tangent axis ô:

$$\sum F_\tau = F_{TP} + G \cdot \sin\alpha - \Phi^Y \cdot \sin\alpha - \Phi^X \cdot \cos\alpha + R_{12} \cdot \cos\delta \mp F_{TP}^{12} \cdot \sin\delta = 0 \quad (17)$$

Sum of applied moments with respect to the point C:

$$\sum M_C = M_{NH} + M_{TP}^C - M_{TP}^K - F_{TP} \cdot r_b = 0 \quad (18)$$

Friction force of grip F_{TP} is evaluated with formula 19 and tangential force $F_ô$ is evaluated with formula 17.

$$F_{TP} = -G \cdot \sin\alpha + \Phi^Y \cdot \sin\alpha \pm F_{TP}^{12} \cdot \sin\delta - R_{12} \cdot \cos\delta + \Phi^X \cdot \cos\alpha \quad (19)$$

The diagram which allows to analyze the conditions of the inertial runner rolling on the inner race for the researched experimental model with central position of the spider (focal length is c_1=0,038) is presented on Figure 2 in polar coordinates, which improves the visualization of sliding zone analysis. Rolling motion of the runner takes place in case of excess of forces of gripping of the runner with the inner track $F_{ôô}$ over resistance force to rolling motion of the runner $F_ô$ (i.e. in places of domination of the solid line over the hatch) and ends in critical values of angle coordinates (of angle φ) at $F_ô$=$F_{ôô}$, otherwise, along with the rolling one can observe the phenomenon of slippage (frictional sliding and skidding) of the runner relating the inner race (in places where the hatch is over the solid line) [9, 10]. Both of these phenomena are observed at exceeding of resistant forces to the runner rolling $F_ô$ over the traction of the runner with the inner race, meanwhile the normal reaction to the inner race N that is a part of $F_ô$ and $F_{ôô}$ and takes different values depending upon the angle δ, which allows to determine definitely which of the listed phenomenon takes place in this or that moment of time.

The analysis of the diagram curves at Figure 11 shows, that when putting the spider axis in the center of the elliptic inner race, at correlation of the values of ellipse semiaxes λ=a/b=0,86, slippage will be observed at 115°≤φ≤147,5° and 295°≤φ≤325° and at 35°≤φ≤65° and 212,5°≤φ≤245° (in places where broken line is over the solid one). Elongation arc of pure rolling of the inertial runner corresponds to 235°.

The length of slippage angle strips of 125°, at constant angle rate of the spider roll ω, is explained with substantial eccentricity e=0,5 of elliptic inner race, which is enveloped by the runner that either speeds up with slippage (at increasing the current radius of point C moving) or skids (at decreasing of the current radius of point C rotating).

To make complete analysis of the strip of the inertial runner slippage on the surface of the inner race, similarly to Figure 11, we will make diagrams of changing of angle strips of slippage for values of the focal length of the inner race c_2=0,045 (Figure 12,a) and c_3=0,06 (Figure 12,b).

Using the methodology of joint analysis of two- and three-dimensional diagrams of functions with the help of MathCAD software product we will make three-dimensional diagram (Figure 13) of changing forces of binding F_{TP} of the runner with the surface of the elliptic inner race and the sum of all tangential forces $F_ô$, operating in the contact point of the inertial runner with the inner race in the function of turning angle of the spider φ and focal length "c".

The diagram give the opportunity to follow visually the clear tendency to increasing the zones of slippage at focal length increase.

The work was performed under the project" Technology of separate making concretes using natural and Anthropogenic raw naterials" (grant of ministry of education and science of the republic of Kazakhstan, contract No. 84-210-13, 10.042013).

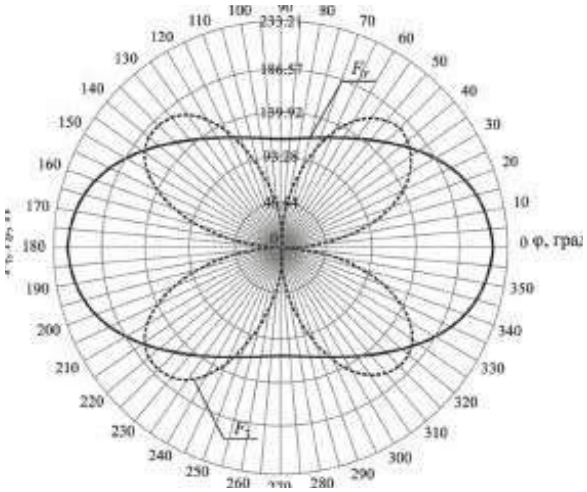

Fig. 11: Dependence of changing the sum of tangential forces $F_ò$ and traction F_{TP} of the runner with the surface of the elliptic inner race upon the angle of the spider turning φ at central position of its axis.

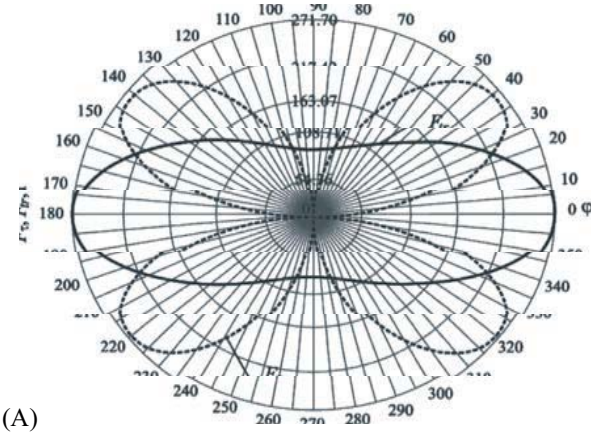

(A)

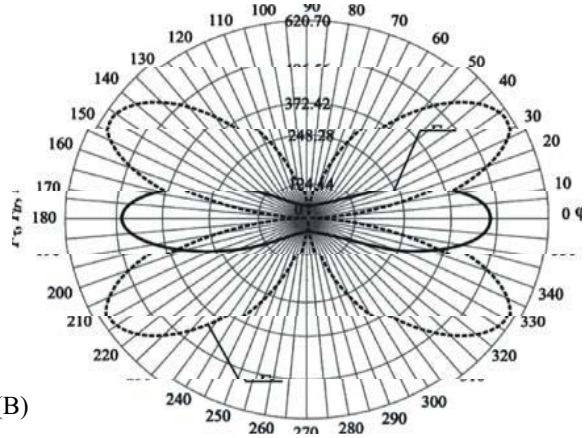

(B)

Fig. 12: Diagram of changing of angle coordinates of the inertial runner slippage on the surface of the elliptic inner race depending upon the focal length "c" : a) c_2=0,045; б) c_3=0,06

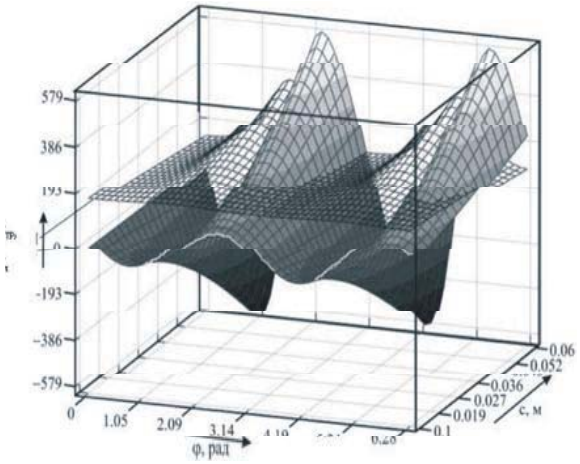

Fig. 13: Dependence of changing forces of binding the runner with the surface of inner race with changing the parameters of the vibroexciter.

Summarizing the written above, we can make the following conclusions:

- The use of a planetary vibroexciter with elliptic inner race gives substantial advantage in generated driving force against an analog vibroexciter, equipped with a round inner race with the same dimensions and initial parameters.
- Selecting the mode of setting the spider axis of a planetary vibroexciter in one of focal points of elliptic inner race leads to the increase of generated driving force, 2.2 times on abscissa axis and 2.4 times on ordinate axis, against the central position of the spider axis. This proves the effectiveness of the elliptic planetary vibroexciter use.
- 1.6 times increase of focal length leads to directly proportional increase of driving force projection on ordinate axis and 2.1 times increase of driving force projection on abscissa axis.
- The use of MathCAD software product for analyzing the working process of the planetary vibroexciter allows by means of three-dimensional plotting to overlap a few linear diagrams in one volumetric, which visually improves the availability of the results of theoretical analysis of the vibroexciter main parameters influence on its dynamic characteristics and reveal major tendencies of their change.
- The use of MathCAD software product allows by means of making 3D diagrams overlap a few linear diagrams in one three-dimensional, which visually improves the availability of the results of theoretical

analysis of influence of critical parameters of the vibroexciter on its dynamic and energy characteristics.

- The increase of eccentricity of elliptic inner race of the planetary vibroexciter over corresponding to focal length c_3=0,06 leads to the decrease of the effectiveness of the vibroexciter because of the increase of supplied power.
- The increase of the mass of the inertial runner and the vibroexciter angular frequency of vibrations also leads to to the increase of supplied power. Their optimal ration can be found on three-dimensional diagrams.
- Angle coordinates of the inertial runner can be determined from the condition of equality of forces of the runner binding with the inner race and tangential forces operating in the point the runner contact with the inner race.
- The developed method of determining and analysis of critical angles of the inertial runner slippage on the surface of the elliptic inner race allows to give recommendations and rationally select design parameters of the elliptic planetary vibroexciter at the designing stage, which can provide sufficient decrease of power intensity, increase of the efficiency and reliability of the vibroexciter.

REFERENCES

1. Ripper Gustavo, Dias Ronaldo, Garcia Guilherme, 10.1.2009. Primary accelerometer calibration problems due to vibration exciters. Elsevier Volume, 42(9): 14-18.
2. Kuznetsov, P.S. and M.V. Doudkin, 2004. Dynamic Analysis of Planetary Vibroexciter with Elliptic Inner Race for Rollers. Machines and Processes in Construction: Coll. of Sc. St. No. 5/ SibABI: 83-87.
3. Chunyu Zhao, Qinghua Zhao, Yimin Zhang and Bangchun Wen, 2011. Synchronization of two non-identical coupled exciters in a non-resonant vibrating system of plane motion, Journal of Mechanical Science and Technology, 25(1): 49-60.
4. Kustarev, G.V., M.V. Dudkin and P.S. Kuznetsov, 2008. Defining Angular Coordinates of Slipping of Inertial Runner of Elliptic Planetary Vibroexciter of Road Machines. Vestnic (Herald) of Moscow Automobile and Road Institute (GTU) 1(12): 15-19.
5. Wen, B.C., H. Zhang and S.Y. Liu, 2010. Theory and Techniques of Vibrating Machinery and Their Applications. Science Press, Beijing, 27(3): 54-61.
6. Temirbekov, Y.S., B.O. Bostanov and M.V. Doudkin, 2006. Determining Force Characteristics of Vibroexciter with Elliptic Inner Race. Vestnik (Bulletin) of ENU. 6(52): 112-117.
7. Zhao, C.Y., D.G. Wang and H. Zhang, 2009. Frequency capture of a vibrating system with two-motor drives rotating in the same direction. Chinese Journal of Applied Mechanics, 26(2): 283-287.
8. Doudkin, M.V. and P.S. Kuznetsov, 2005. Dynamic Analysis of Elliptic Planetary Vibroexciter for Road Vibration Rollers. Journal Vestnik EKSTU (Bulletin of EKSTU, Ust-Kamenogorsk): pp: 7.
9. Seung-Bok Choi, Sung Hoon Ha and Juncheol Jeon October 2, 2012. Vibration Control of Flexible Structures Using Semi-Active Mount. Experimental Investigation, Advances in Vibration Engineering and Structural Dynamics, ISBN 978-953-51-0845-0, Published.
10. Dzholdasbekov, S.U. and Y.S.Temirbekov, July 6 - 8, 2011, London, U.K.. Shock-free Race Track of Road Roller Vibration Exciters, Proceedings of the World Congress on Engineering. Vol III WCE. pp: 25-36.